**GSA Data Repository 2013325**


**Carbon dioxide emission to Earth's surface by deep-sea volcanism**

Satoshi Okumura and Naoto Hirano

**Survey Area off the Japan Trench**


Shipboard multibeam data for the Japan Trench and the NW Pacific areas were obtained during several cruises onboard the R/V Kairei (KR03-07 and KR04-08) and R/V Yokosuka (YK05-06) cruises (Hirano et al., 2006) as the research project "Expedition for petit-spot" carried out by the Japan Agency for Marine-Earth Science and Technology (JAMSTEC), which are supplied from the Deep Sea Research Data Web (http://www.jamstec.go.jp/e/database/). We used the "SeaBeam" system built by L-3 Communications SeaBeam Instruments Inc. to produce the wide-swath contour maps and the acoustic backscatter images of the seafloor at surveying speeds of 12 to 8 knot. The horizontal resolution of the bathymetry data depends on the depth and ship speed. Data quality also depends greatly on the sea state.

The area in the map of Fig. DR1 is approximately 312,000 km$^2$; the surveys covered the area of 36% in the map during the cruises, which is approximately 112,000 km$^2$. The 16,993,496 data gridded in 0.005-min cells are plotted on the depths below sea level. We utilized the Generic Mapping Tools (Wessel and Smith, 1995) and the MB-system (Caress and Chayes, 1996) for filtering, gridding and plotting the data sets.


**Analytical Methods**

For our determination of carbon dioxide and water contents, glassy basalts were doubly polished to make thin sections of 97–145 μm thickness. The chemical compositions of the glasses were analyzed using a wavelength dispersive spectroscopy electron microprobe (JXA-8800M, JEOL Ltd.) (Table DR1). The measurements were performed using a broad beam, 15 kV accelerating voltage, 12 nA beam current, and peak counting time of 10 s. Backscattered electron images obtained by a scanning electron microprobe (S3400N, Hitachi High-Tech. Co.) were converted to binary images in order to determine the volume fraction of bubbles (vesicularity). After EPMA analyses, the thin sections were analyzed with an FT-IR microspectrometer (Nicolet iN-10, Thermo Fisher Scientific Inc.). To determine the carbon dioxide and water contents, absorbances at the 1515 and 1430 cm$^{-1}$ bands for carbon dioxide (carbonate)

(Dixon and Pan, 1995) and at the 3550 cm$^{-1}$ band for water (hydroxyl group) (Dixon et al., 1995) were measured after baseline correction. The concentration of $H_2O$ molecule ($H_2O_m$) was also determined on the basis of the 1630 cm$^{-1}$ absorbance (Dixon et al., 1995). The baseline spectra were obtained by analyzing glass samples, which were heated and devolatilized. For preparation of devolatilized glass samples, sample chips were crushed and powdered, and then heated in a furnace using the platinum wire loop method (Pupier et al., 2008) at a temperature of 1350 °C. The baseline spectra obtained from the devolatilized glass samples showed no absorption for the bands corresponding to carbon dioxide and water. The carbon dioxide and water contents were calculated from measured absorbances, thin section thickness, glass density, and molar absorptivities on the basis of the Lambert-Beer's law. The thickness of thin sections was measured using a digital micrometer, and the glass density was calculated from the relationship between glass density and water content (Ohlhorst et al., 2001).

**References**

Caress, D.W., and Chayes, D.N., 1996, Improved processing of Hydrosweep DS multibeam data on the R/V Maurice Ewing: Marine Geophysical Researches, v. 18, p. 631–650.

Dixon, J.E., and Pan, V., 1995, Determination of the molar absorptivity of dissolved carbonate in basaltic glass: The American Mineralogist, v. 80, p. 1339–1342.

Dixon, J.E., Stolper, E.M., and Holloway, J.R., 1995, An experimental study of water and carbon dioxide solubilities in mid-ocean ridge basaltic liquids. Part I: Calibration and solubility models: Journal of Petrology, v. 36, p. 1607–1631.

Hirano, N., Takahashi, E., Yamamoto, J., Abe, N., Ingle, S., Kaneoka, I., Hirata, T., Kimura, J., Ishii, T., Ogawa, Y., Machida, S., and Suyehiro, K., 2006, Volcanism in response to plate flexure: Science, v. 313, p. 1426–1428.

Hirano, N., Koppers, A.A.P., Takahashi, A., Fujiwara, T., and Nakanishi, M., 2008, Seamounts, knolls and petit spot monogenetic volcanoes on the subducting Pacific Plate: Basin Research, v. 20, p. 543–553.

Lange, R.L., and Carmichael, I.S.E., 1990, Thermodynamic properties of silicate liquids with emphasis on density, thermal expansion and compressibility: Modern methods of igneous petrology: understanding magmatic processes, Reviews in Mineralogy, v. 24, p. 24–64.

Ohlhorst, S., Behrens, H., and Holtz, F., 2001, Compositional dependence of molar absorptivities of near-infrared OH- and $H_2O$ bands in rhyolitic to basaltic glasses: Chemical Geology, v. 174, p. 5–20,

doi:10.1016/S0009-2541(00)00303-X.

Pupier, E., Duchene, S., and Toplis, M., 2008, Experimental quantification of plagioclase crystal size distribution during cooling of a basaltic liquid: Contributions to Mineralogy and Petrology, v. 155, p. 555–570, doi:10.1007/s00410-007-0258-9.

Wessel, P., and Smith, W.H.F., 1995, New version of the Generic Mapping Tools released: EOS, Transactions American Geophysical Union, v. 76, n. 329.
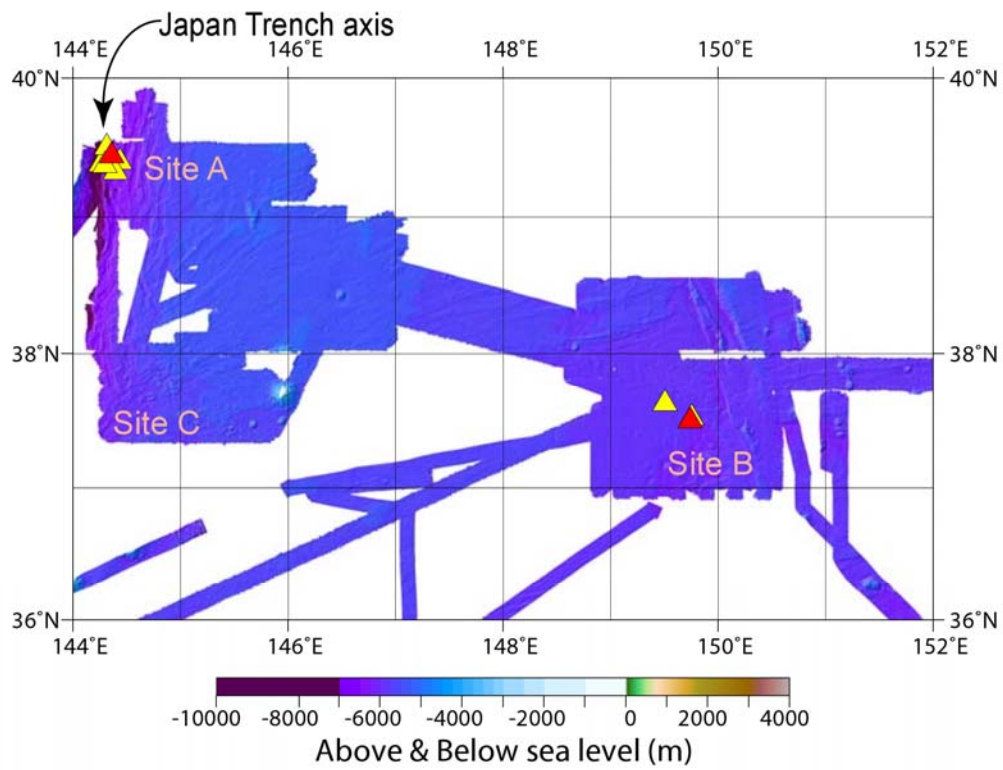
**Figure DR1.** Shipboard detailed bathymetry. The red symbols represent sampling points for rocks investigated in this study (Sites A and B). Site C is another area implying the presence of petit-spots, probably more than 90 young volcanoes (Hirano et al., 2008).

TABLE DR1. CHEMICAL COMPOSITION AND VESICULARITY OF GLASSY BASALTS

| Site | SiteA | | SiteA | | SiteB | | SiteB | |
|---|---|---|---|---|---|---|---|---|
| Cruse | KR07-06 | | KR07-06 | | KR04-08 | | KR04-08 | |
| Sampling | 7K#387R09-1 | | 7K#387R09-2 | | D07 | | D08 | |
| (wt%) | | | | | | | | |
| $SiO_2$ | 47.93 | (0.20)* | 48.03 | (0.22) | 47.74 | (0.25) | 46.23 | (0.25) |
| $TiO_2$ | 3.10 | (0.06) | 3.10 | (0.06) | 2.92 | (0.08) | 3.06 | (0.06) |
| $Al_2O_3$ | 11.83 | (0.09) | 11.97 | (0.11) | 12.98 | (0.15) | 13.00 | (0.14) |
| FeO | 9.54 | (0.16) | 9.48 | (0.17) | 10.45 | (0.15) | 10.30 | (0.19) |
| MnO | 0.12 | (0.02) | 0.15 | (0.04) | 0.12 | (0.03) | 0.16 | (0.03) |
| MgO | 6.87 | (0.07) | 6.83 | (0.07) | 6.90 | (0.07) | 5.76 | (0.11) |
| CaO | 8.56 | (0.04) | 8.61 | (0.08) | 9.45 | (0.08) | 10.71 | (0.09) |
| $Na_2O$ | 3.47 | (0.09) | 3.47 | (0.06) | 3.77 | (0.09) | 4.08 | (0.17) |
| $K_2O$ | 5.05 | (0.05) | 5.03 | (0.04) | 2.82 | (0.02) | 3.11 | (0.04) |
| $P_2O_5$ | 1.24 | (0.04) | 1.24 | (0.06) | 1.06 | (0.05) | 1.40 | (0.05) |
| Total | 97.71 | | 97.93 | | 98.22 | | 97.83 | |
| $H_2O_t$ | 1.00 | (0.04) | 0.98 | (0.04) | 0.94 | (0.03) | 0.89 | (0.01) |
| OH | 0.79 | (0.08) | 0.74 | (0.04) | 0.72 | (0.05) | 0.75 | (0.02) |
| $H_2O_m$ | 0.21 | (0.07) | 0.24 | (0.01) | 0.22 | (0.04) | 0.14 | (0.02) |
| $CO_2$ (ppm) | 547 | (110) | 552 | (20) | 773 | (106) | 949 | (76) |
| Vesicularity (vol%) | 22 | | 31 | | 43 | | 38 | |
| Magma density[†] | 2640 | | 2640 | | 2680 | | 2680 | |

* The parentheses represent standard deviation (1ξ).

[†] Magma density was calculated at a temperature of 1200°C (Lange and Carmichael, 1990).